Fuel Efficiency Optimization in Adaptive Cruise Control: A Comparative Study of Model Predictive Control-Based Approaches

Optical Materials: X 8 (2020) 100058

Contents lists available at ScienceDirect

Optical Materials: X

journal homepage: www.journals.elsevier.com/optical-materials-x

Design of 1D photonic crystals for colorimetric and ratiometric refractive index sensing

Simone Normani [a], Nicholas Dalla Vedova [a], Guglielmo Lanzani [a,b], Francesco Scotognella [a,b], Giuseppe M. Paternò [a,*]

[a] Istituto Italiano di Tecnologia, Center for Nano Science and Technology, Via Giovanni Pascoli, 70, 20133, Milano, Italy
[b] Department of Physics, Politecnico di Milano, Piazza L. Da Vinci 32, 20133, Milano, Italy

ARTICLE INFO

Keywords:
Photonic crystals
Distributed Bragg reflectors
Refractive index
Sensing

ABSTRACT

Photonic crystals can be employed effectively as simple and low-cost colorimetric sensors for monitoring variation in the environmental refractive index. In most cases, the photonic colorimetric approach relies on the use of porous and permeable materials to highlight refractive index (RI) modulation, although a fine control over the size distribution and free volume can be complex to achieve. Here, we propose nonporous low-layer count distributed Bragg reflectors (DBRs) as simple optical devices for colorimetric refractive index sensing. In our feasibility study, we simulated the reflectance of DBRs consisting of two to five SiO_2/TiO_2 bilayers upon variation of the external refractive index. We found that the 2-bilayers sample exhibits the highest sensitivity to RI variations, and identified the ratio between the first and third order reflectance intensity as simple yet efficient ratiometric parameter to discern analytes with different refractive indices. This approach can provide a promising perspective for the development of cheap and portable devices for environmental detection of a wide range of substances.

1. Introduction

Photonic colorimetric sensing represents a simple and effective approach that can be useful for monitoring changes in the surrounding environment, such as humidity and temperature [1,2], as well as for the identification of a large variety of substances, ranging from liquids/vapours to bio analytes [3–8]. The structural reflection colour of photonic crystals (PhCs) originates from the periodic arrangement along the three spatial dimensions of materials with different refractive indices [9,10], which gives rise to a forbidden band for photons, the so-called photonic band gap (PBG). This, in turn, can be exploited as simple yet effective colorimetric probe/parameter that responds to those external and environmental stimuli that are able to modify the photonic lattice spacing and/or refractive index (RI) contrast [11–17].

For instance, the infiltration of liquids and capillary condensation of gases in mesoporous one-dimensional PhCs, also known as Distributed Bragg Reflectors (DBRs), has been widely utilized for sensing purposes [18–20], while the large surface area in these porous systems can also enable biosensing applications [21–23]. However, the precise control over pore size distribution that is essential for analyte percolation and for driving analyte selectivity in these devices is in general very difficult to achieve with scalable fabrication techniques (*i.e.* solution-based processes and radio-frequency sputtering, among others), while this can be usually attained by means of highly complex fabrication procedures [24]. Furthermore, full sensing reversibility results to be limited in some cases, owing to the stagnancy of the analytes or spurious external substances, within the porous microstructure. Therefore, while porosity represents usually a great advantage in colorimetric photonic sensing, alternative approaches relying on non-complex photonic structures are also worth exploring. For instance, a ratiometric detection scheme should in principle enhance measurement reliability and sensitivity, as in this way any noise/signal fluctuation would be compensated [25].

Here, we propose simple low-layer count DBRs as nonporous and cost-efficient platforms to track environmental refractive index variations. In order to assess our idea, we developed a simulation program which permits to calculate rapidly the reflection spectra of the device under different refractive conditions and for varying number of layers, thus providing an efficient theoretical tool for identifying the optimal DBR design and, importantly, the most significant absolute and

* Corresponding author.
E-mail address: giuseppe.paternò@iit.it (G.M. Paternò).

https://doi.org/10.1016/j.omx.2020.100058
Received 24 June 2020; Received in revised form 8 July 2020; Accepted 9 July 2020
Available online 25 July 2020

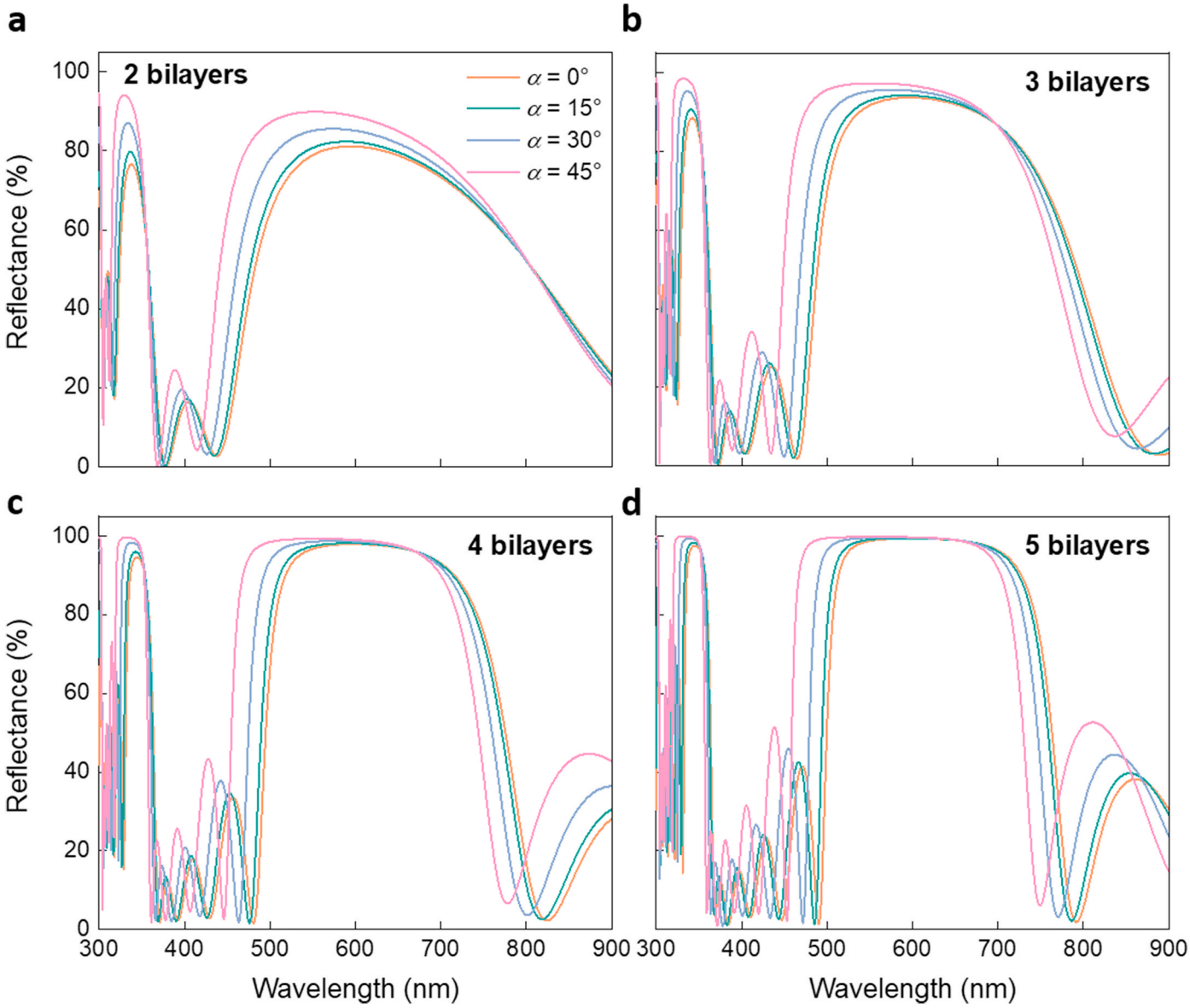

Fig. 1. Simulated reflection spectra of SiO_2–TiO_2 DBRs with (a) 2, (a) 3, (a) 4, and (d) 5 pairs of layers, at various incidence angles, α.

ratiometric spectral parameters to monitor upon variation of the RI contrast. In particular, we envisage DBRs fabrication by means of radio frequency (RF) sputtering, as it provides reliable thickness and a low/controlled porosity while being a relatively easy, cheap and scalable production process. The final goal of our study is to provide a simple label-free colorimetric RI sensor capable to detect a broad range of substances while operating in the visible range, which does not require any porous microstructure and/or complex micro/nanofabrication procedures to monitor environmental RI variations.

2. Methods

A simulation routine was coded in *Wolfram Mathematica*, using the transfer matrix formalism to calculate the reflection spectra of two-material DBRs [26]. The program was designed in a way that it was possible to obtain quick estimates of transmission spectra by defining the thickness, porosity and refractive index dispersion curves of the materials, as well as the dispersion curve of the external refractive index, number of layers, angle of incidence of the hypothetical probe beam, and wavelength sampling interval. The effects of porosity on the refractive index were defined according to the Maxwell-Garnett model [27]. The refractive index dispersion equations of the different substances were obtained from literature [28]. The program was set up as to use a discrete, point-by-point calculation of the reflection values according to the sampling interval. The reference structure of choice was a SiO_2–TiO_2 1D photonic crystal with layer thicknesses respectively 100 nm and 60 nm for the two glasses, in order to obtain a PBG centred at 600 nm. The program was set to simulate the reflection spectra from 300 nm to 900 nm with a 1 nm sampling interval, allowing to investigate not only the first-order PBG, but also the third order. The simulations were run for different sets of conditions and the spectra were collected and compared. The first- and third-order PBG maximum reflection values and positions were identified as viable probe quantities of the device.

3. Results and discussion

First, we calculated the reflectance spectra for the DBRs exposed to vacuum (RI = 1) consisting of 2, 3, 4 and 5 SiO_2/TiO_2 bilayers, and for incidence angles of 0° (normal incidence), 15°, 30°, and 45° (Fig. 1).

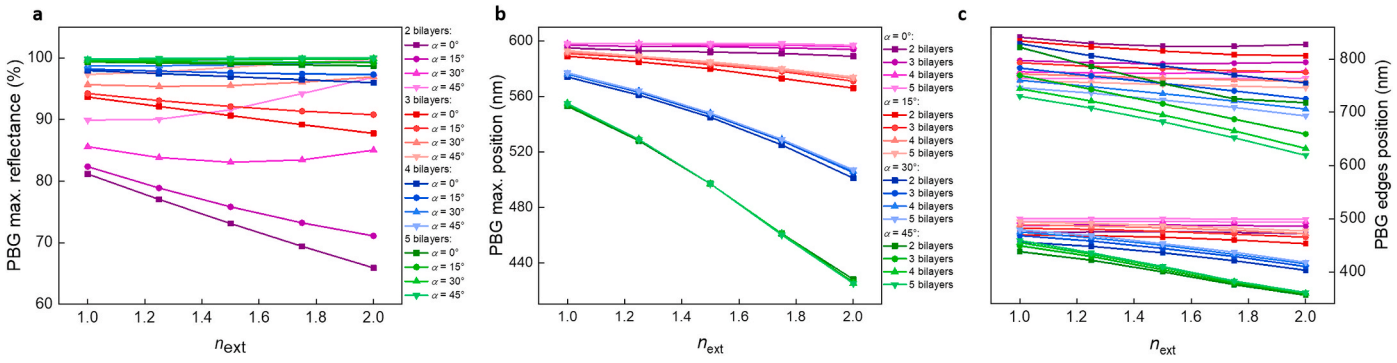

Fig. 2. PBG (a) maximum reflection value, (b) maximum position, and (c) edges position as a function of the external medium refractive index, for DBRs with different number of layers and at different incidence angles.

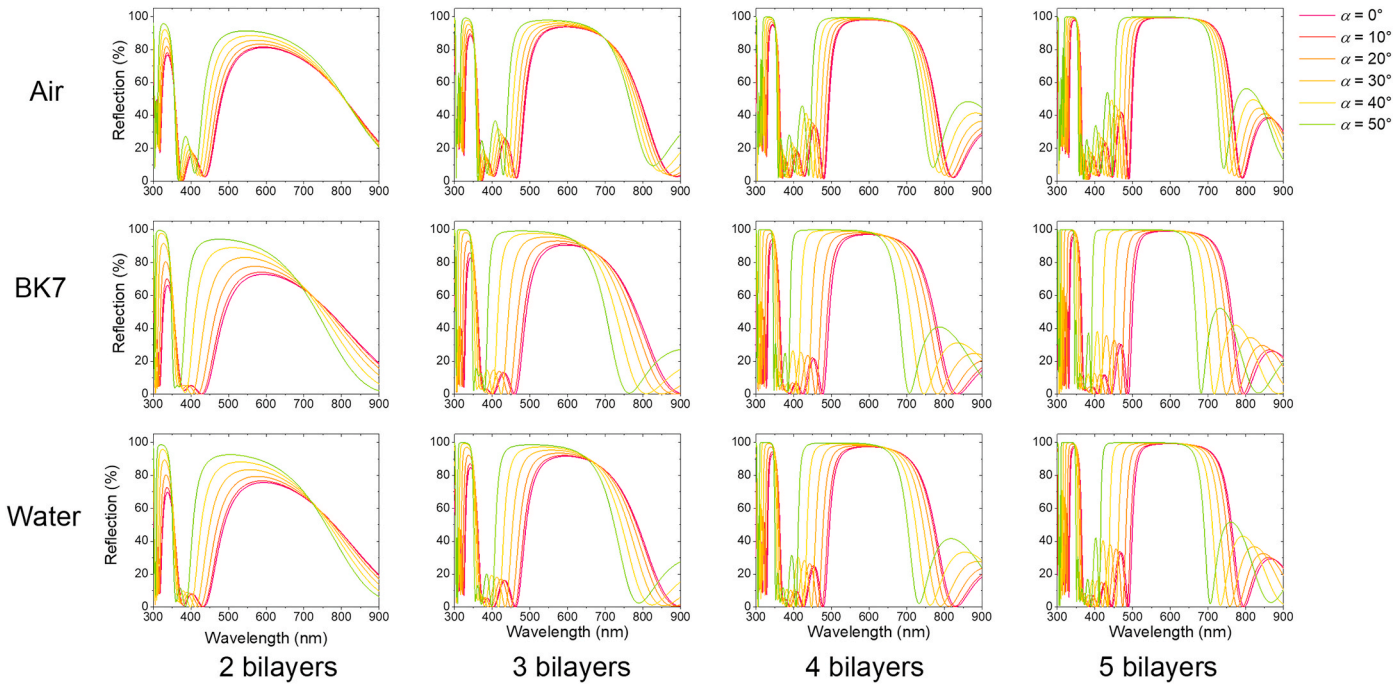

Fig. 3. Reflection spectra of DBRs with different layer counts and at various angles of incidence, calculated upon exposure to substances with known refractive index dispersion: air, Cargille BK7 matching liquid, and water.

This serves to assess the intrinsic properties of the DBRs, in terms of photonic dispersion in absence of any substance in the surrounding environment, thus providing a control measurement. We can observe the PBG centred at 600 nm for all the crystals, while the third-order PBG arising from the third-harmonic destructive interface appears at 340 nm. This latter reflection is positioned at 340 nm and not at 200 nm simply due to the sensible increase in the refractive index of the glasses at lower wavelengths compared to that at 600 nm. The plots show very clearly the well-known dependence of the first-order PBG maximum $R_{(1)}$ on the number of layers N:

$$R_{(1)} = 100 \cdot \left(\frac{\left(\frac{n_{SiO_2}}{n_{TiO_2}}\right)^{2N} - 1}{\left(\frac{n_{SiO_2}}{n_{TiO_2}}\right)^{2N} + 1} \right)^2 \quad (1)$$

In addition, one can also note the shift upon increase of the incidence angle that determines the photonic dispersion of our systems, in agreement with the Bragg-Snell law [29,30]. From these data, we can already identify at least five possible parameters that can be considered to track the RI variation namely: i) the PBG spectral position, the reflectance maximum of the ii) first- and iii) third-order peaks, iv) their intensity ratio and v) the photonic dispersion (reflectance spectrum *vs.* incidence angle). We will from now on refer to the first-order PBG maximum reflectance and position as $R_{(1)}$ and $\lambda_{(1)}$ respectively, and likewise to the third-order equivalents with $R_{(3)}$ and $\lambda_{(3)}$.

We then calculated the reflectance spectrum for refractive index variation ranging from 1 to 2 (step = 0.25) at the four incidence angles (0°, 15°, 30°, and 45°) and layers count (2, 3, 4, 5 bilayers). The $R_{(1)}$ and $\lambda_{(1)}$ values, as well as the half-maximum first-order PBG edge positions, were then plotted as a function of the external refractive index (Fig. 2), providing in-fact a first figure of merit of the optical response of the device. Increasing the number of bilayers leads to $R_{(1)}$ values tending asymptotically to 100% (Fig. 2a), therefore rendering such parameter almost insensible to external stimuli. On the other hand, low-layer counts DBR exhibiting relatively lower $R_{(1)}$ values are indeed very sensitive to n_{ext}, as in this case the topmost layer interface with the external medium has a comparatively greater importance to the response of the device, and the PBG is less defined and thus more susceptible to external variation than the high-layer count counterparts. Passing to the DBRs dispersion properties as a function of n_{ext} (Fig. 2b), we note that PBG

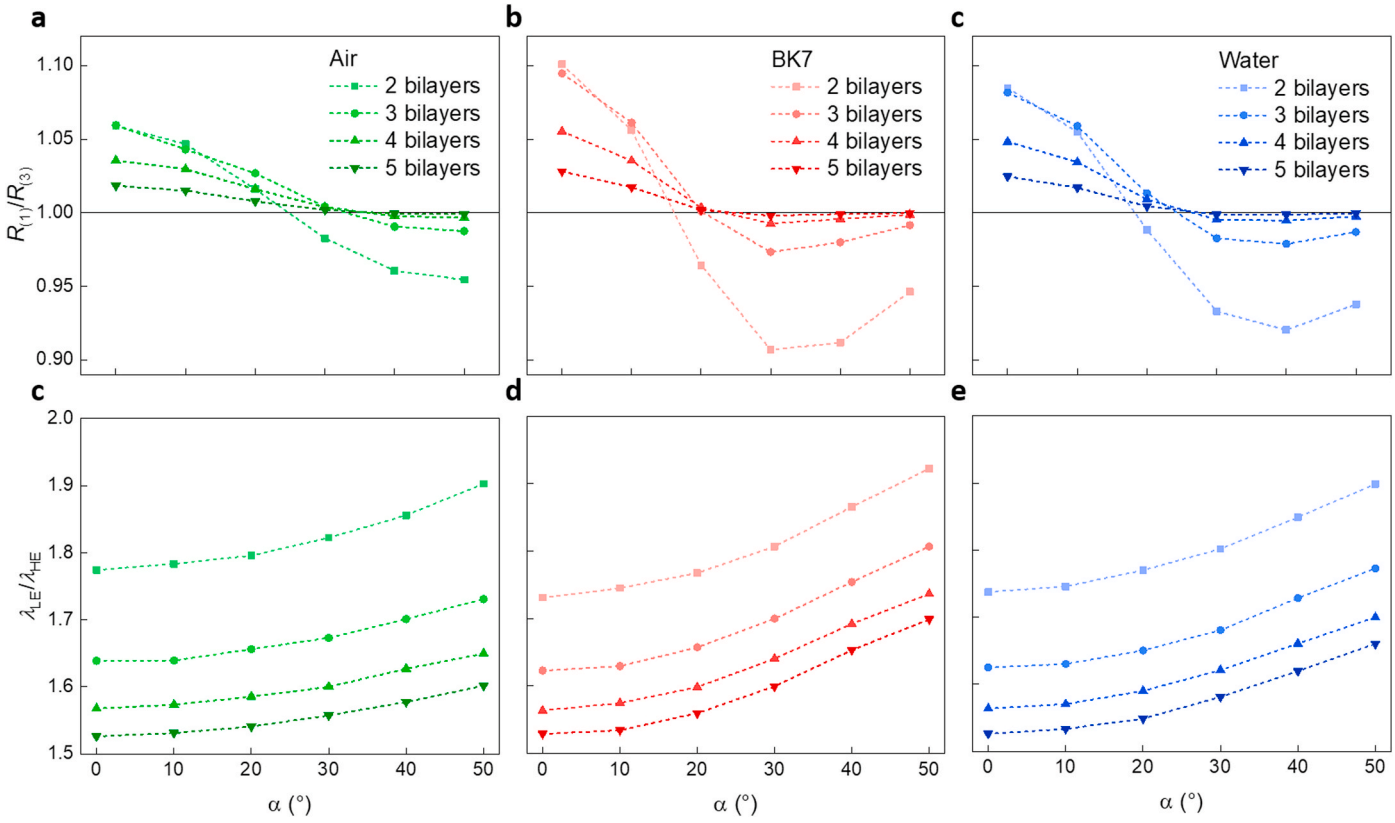

Fig. 4. First- and third-order reflection ratio as a function of the incidence angle α for DBRs surrounded by the three reference substances: (a) air, (b) BK7 matching liquid and (c) water. Plot of the ratio between low-energy PBG edge position (λ_{LE}) and high-energy PBG edge position (λ_{HE}), as a function of the incidence angle α for DBRs surrounded by the three reference substances: (d) air, (e) BK7 matching liquid and (f) water.

position *vs.* the refractive index is mostly not affected by the layer count. A simple explanation for such effect is provided by the Snell's law of refraction, which states that only the very first interface is involved in the refractive process. On the other hand, the photonic dispersion can be still used as sensing parameter, as the variation of the spectral parameters become more evident at higher incidence angles by virtue of the aforementioned Snell's law. Finally, we also plotted the PBG low- and high-energy edge positions (from here on referred to as λ_{HE} and λ_{LE} respectively) as a function of n_{ext} and incidence angle α (Fig. 2c), noting that this parameter can be more sensitive to the external refractive index dispersion than $\lambda_{(1)}$, thanks to the higher local slope values. Furthermore, this behaviour suggests the possibility to use such devices as tuneable optical band-pass or notch filters, in which the tuning element is simply the surrounding medium dispersion.

While these simulations are useful to provide an understanding of the devices response to the environment refractive index change in the close proximity of the PBG centre, the differential behaviour of the first- and –third-order bands can potentially provide additional information on the refractive index at different wavelengths, with the outlook of building up a ratiometric sensor. To test this hypothesis, we simulated the optical behaviour of the DBRs upon exposure to three possible analytes that do not absorb in the investigated spectral range, while exhibiting different optical properties, namely air [31], water [32] (at room temperature) and Cargille BK7 matching liquid [33] (Fig. 3). From the qualitative point of view, we can see that whereas the absolute values of $\lambda_{(1)}$ and $\lambda_{(3)}$ do not exhibit any significant dependence on the number of layers, essentially confirming the data shown in Fig. 2b, $R_{(1)}/R_{(3)}$ and $\lambda_{HE}/\lambda_{LE}$ show a differential behaviour as a function of the incident angle α and the investigated substance. Interestingly, this suggests that a ratiometric sensing approach can be in principle adopted.

To evaluate such an aspect from the quantitative point of view, we plotted these latter ratiometric quantities as a function of the incidence angle (Fig. 4). We can clearly appreciate that the dispersion curves for the three substances differ from one another and, importantly, depend strongly on the layer count. Starting from $R_{(1)}/R_{(3)}$ (Fig. 4a,b,c), the amplitude of the fluctuation around the unity increases by decreasing the number of layers. For instance, if we focus on the 2-bilayers DBR, we can see that the fluctuation is sensibly different among the investigated substances both in terms of amplitude (10%, 20% and 15% for air, BK7, and water, respectively) and shape. In particular, $R_{(1)}/R_{(3)}$ in this case exhibits a higher slope variation vs. α than the higher-count samples, a quantity that also depends on the nature of the substance. This in fact can represent a valid and robust sensing parameter for the colorimetric discrimination of substances with relatively similar refractive index dispersions. Again, this can be possible in low-layer count DBR, in which the reflectance intensity and the $R_{(1)}/R_{(3)}$ parameter can be modulated appreciably upon variation of the environmental refractive index. Another useful quantity can be identified in the ratio between the positions of the PBG low- and high-energy edges, $\lambda_{LE}/\lambda_{HE}$. As one can see in Fig. 4d,e,f, this parameter is less sensitive to the number of layers than $R_{(1)}/R_{(3)}$, as the slope of the curve does not change drastically with increasing layer count. However, $\lambda_{LE}/\lambda_{HE}$ can still exhibit different dispersion curves *vs.* the examined substances and, in addition, can provide a reliable parameter in DBR with high-layer counts due to the highly defined PBG edges in these samples.

It should be pointed out that, while these estimates are valid for a freestanding periodic structure, the presence of the substrate is expected contribute to the linewidth. This is a critical aspect in the view to fabricate these devices via RF sputtering, since this method allows deposition of materials in a wide range of substrates [34]. To minimize

any effect of the substrate on the optical read-out, a high transparency in the spectral region of interest is an important requisite. This can be achieved usually by either choosing a fitting substrate material for a specific DBR, or tailoring the DBR properties according to the available choice of substrate materials. Alternatively, one can choose a material with a refractive index that matches the one of the analyte, to reduce the contributions of the substrate/environment interface. A higher number of DBR layers also reduces the relative contribution of the substrate to the overall spectral features, therefore a compromise between DBR sensitivity and low substrate contributions should be evaluated when designing the device.

Finally, we proceed to the evaluation of the theoretical resolution limits of our DBRs. With this in mind, we calculated the fluctuations in the optical properties of the devices as a function of the intrinsic fabrication parameters that are mostly affected by errors/imperfections during the manufacturing process: layer thickness and porosity. We selected radiofrequency sputtering as a reference fabrication technique, as it usually allows reliable control over the layer thickness and low porosity, while being a relatively easy, cheap and fast method of fabrication [35]. In this case, one may reasonably expect thickness fluctuations within 1 nm for each layer, and porosity under 5% for both SiO_2 and TiO_2 [36]. Therefore, to obtain the tolerance limits, we performed separate simulations with thickness and porosity values within those extremes. Focusing on the 2-bilayers configuration that shows the most sensible response against variations in the n_{ext}, we found that a 1 nm fluctuation corresponds to a maximum error of 0.027 on refractive index, whereas if the porosity ranges between 0% and 5% the $R_{(1)}$ value varies by 0.9%, corresponding to a 0.06 interval in refractive index. Note that another advantage of this method is that the device response is approximately linear, which makes conversion straightforward, and therefore the error can be easily propagated. In summary, given these extremes the minimum discernible refractive index variation would be about 0.09, a value that is essentially dominated by the uncertainty on porosity. The same procedure was employed to estimate the reliability of the PBG edge positions. Also in this case, porosity contributes the most to the estimated refractive index uncertainty: in particular, an error of 1 nm on layer thickness accounts for minimum discernible refractive index fluctuations of 0.05 and 0.12 at λ_{HE} and λ_{LE}, respectively, while porosity leads to variations of 0.08 at λ_{HE} and 0.20 at λ_{LE}. These results impose an important *caveat* to the use of such parameters. In particular, while the PBG edge positions can be in general easily assessed, they also entail greater intrinsic uncertainty to the RI estimation, therefore might be considered as a complementary parameter.

4. Conclusions

In summary, we have reported on the design of simple colorimetric devices for refractive index sensing applications, which do not require neither a micro/nanoporous structure nor complex geometries. We focused on a simple DBR architecture that usually ensures relatively high colorimetric response against a wide range of analytes, while being simple and low-cost devices that can be fabricated from scalable processes. Our data indicate that low-layer count DBRs represent an interesting option for monitoring external refractive index variations, due to the better responsivity of the amount of reflected light against external stimuli. Specifically, we identified a ratiometric parameter, namely the ratio between the first- and third order reflectance intensity ($R_{(1)}/R_{(3)}$), whose photonic dispersion permits to obtain a reliable optical fingerprint of the analyte, as well as a complementary parameter in the low-to-high energy PBG edge position ratio ($\lambda_{LE}/\lambda_{HE}$) which can be used to provide additional information on the dispersion curve. Finally, we evaluated the resolution limits of the proposed devices, observing that proper fabrication is the key element that affects such a parameter, as we found that the uncertainty on the thickness and porosity of the deposited layers is determinant for the resolution of the refractive index value detection. In this context, while such systems can be quite easily fabricated by many different techniques, radiofrequency sputtering is the most appealing due to the high degree of control on these critical properties. In addition, process scalability can enable applications of this simple low-count stacks in packaging, *i.e.* to track the presence of food contaminants from the production site to the consumers.

Author contribution

S.N: conceived the work. performed the simulations, writing of the paper, N.D.V: contributed to paper writing and data analysis, writing of the paper, G L: writing of the paper, F.S: helped in the analyzation of the simulations, writing of the paper, G.M.P: conceived the work, supervised the work, writing of the paper.

Data availability

The data that support the findings of this study are available from the corresponding author upon reasonable request.

Declaration of competing interest

The authors declare that they have no known competing financial interests or personal relationships that could have appeared to influence the work reported in this paper.

Acknowledgements

This work has been supported by Fondazione Cariplo, grant n° 2018–0979. F.S. thanks the European Research Council (ERC) under the European Union's Horizon 2020 research and innovation programme (grant agreement No. [816313]).

References

[1] H. Wang, K.Q. Zhang, Sensors 13 (2013) 4192.
[2] D. Kou, W. Ma, S. Zhang, J.L. Lutkenhaus, B. Tang, ACS Appl. Mater. Interfaces 10 (2018) 41645.
[3] F. Gao, Q. Liao, Z.Z. Xu, Y.H. Yue, Q. Wang, H.L. Zhang, H.B. Fu, Angew. Chem. Int. Ed. 49 (2010) 732.
[4] B. Ye, F. Rong, H. Gu, Z. Xie, Y. Cheng, Y. Zhao, Z. Gu, Chem. Commun. 49 (2013) 5331.
[5] P. Lova, G. Manfredi, L. Boarino, A. Comite, M. Laus, M. Patrini, F. Marabelli, C. Soci, D. Comoretto, ACS Photonics 2 (2015) 537.
[6] G.M. Paternò, L. Moscardi, S. Donini, D. Ariodanti, I. Kriegel, M. Zani, E. Parisini, F. Scotognella, G. Lanzani, J. Phys. Chem. Lett. 10 (2019) 4980.
[7] G.M. Paterno, L. Moscardi, S. Donini, A.M. Ross, S.M. Pietralunga, N. Dalla Vedova, S. Normani, I. Kriegel, G. Lanzani, F. Scotognella, Faraday Discussions, Roy. Soc. Chem. (2020), https://doi.org/10.1039/D0FD00026D. In press, https://pubs.rsc.org/en/content/articlelanding/2020/fd/d0fd00026d/unauth#!divAbstract.
[8] G.M. Paternò, N. Barbero, S. Galliano, C. Barolo, G. Lanzani, F. Scotognella, R. Borrelli, J. Mater. Chem. C 6 (2018) 2778.
[9] E. Yablonovitch, Phys. Rev. Lett. 58 (1987) 2059.
[10] A. Chiasera, F. Scotognella, L. Criante, S. Varas, G. Della Valle, R. Ramponi, M. Ferrari, Sci. Adv. Mater. 7 (2015) 1207.
[11] G.M. Paternò, C. Iseppon, A. D'Altri, C. Fasanotti, G. Merati, M. Randi, A. Desii, E. A.A. Pogna, D. Viola, G. Cerullo, F. Scotognella, I. Kriegel, Sci. Rep. 8 (2018) 3517.
[12] G.M. Paternò, L. Moscardi, I. Kriegel, F. Scotognella, G. Lanzani, J. Photon. Energy 8 (2018) 1.
[13] F. Scotognella, G.M. Paternò, I. Kriegel, S. Bonfadini, L. Moscardi, L. Criante, S. Donini, D. Ariodanti, M. Zani, E. Parisini, G. Lanzani, in: S. Taccheo, M. Ferrari, J.I. Mackenzie (Eds.), Fiber Lasers Glas. Photonics Mater. Through Appl. II, SPIE, 2020, p. 53.
[14] S. Heo, A. Agrawal, D.J. Milliron, Adv. Funct. Mater. 29 (2019), 1904555.
[15] E. Redel, J. Mlynarski, J. Moir, A. Jelle, C. Huai, S. Petrov, M.G. Helander, F. C. Peiris, G. von Freymann, G.A. Ozin, Adv. Mater. 24 (2012) OP265.
[16] P. Lova, P. Giusto, F. Di Stasio, G. Manfredi, G.M. Paternò, D. Cortecchia, C. Soci, D. Comoretto, Nanoscale 11 (2019) 8978.
[17] V. Robbiano, G.M. Paternò, A.A. La Mattina, S.G. Motti, G. Lanzani, F. Scotognella, G. Barillaro, ACS Nano 12 (2018) 4536.
[18] M.C. Fuertes, S. Colodrero, G. Lozano, A.R. González-Elipe, D. Grosso, C. Boissière, C. Sánchez, G.J. de A.A. Soler-Illia, H. Míguez, J. Phys. Chem. C 112 (2008) 3157.
[19] N. Hidalgo, M.E. Calvo, M.G. Bellino, G.J.A.A. Soler-Illia, H. Míguez, Adv. Funct. Mater. 21 (2011) 2534.
[20] S.Y. Choi, M. Mamak, G. Von Freymann, N. Chopra, G.A. Ozin, Nano Lett. 6 (2006) 2456.

[21] L.D. Bonifacio, D.P. Puzzo, S. Breslav, B.M. Willey, A. McGeer, G.A. Ozin, Adv. Mater. 22 (2010) 1351.
[22] L.D. Bonifacio, G.A. Ozin, A.C. Arsenault, Small 7 (2011) 3153.
[23] V. González-Pedro, M.E. Calvo, H. Míguez, Á. Maquieira, Biosens. Bioelectron. X 1 (2019), 100012.
[24] M.M. Hawkeye, M.J. Brett, Adv. Funct. Mater. 21 (2011) 3652.
[25] N. Kumawat, M.M. Varma, Appl. Phys. Lett. 101 (2012), 191103.
[26] J.D. Joannopoulos, S.G. Johnson, J.N. Winn, R.D. Meade, Photonic Cryst. Molding Flow Light, second ed., 2011.
[27] T.C. Choy, Effective Medium Theory: Principles and Applications, Oxford University Press, 2015.
[28] https://refractiveindex.info/. (Accessed 5 April 2020). Accessed.
[29] G. Mayonado, S.M. Mian, V. Robbiano, F. Cacialli, 2015 *Conf.* Lab. Instr. Beyond First Year, American Association of Physics Teachers, 2015, pp. 60–63.
[30] V. Robbiano, G.M. Paternò, G.F. Cotella, T. Fiore, M. Dianetti, M. Scopelliti, F. Brunetti, B. Pignataro, F. Cacialli, J. Mater. Chem. C 6 (2018) 2502.
[31] P.E. Ciddor, Appl. Optic. 35 (1996) 1566.
[32] A.H. Harvey, J.S. Gallagher, J.M.H.L. Sengers, J. Phys. Chem. Ref. Data 27 (1998) 761.
[33] https://www.cargille.com/matching-liquids/. (Accessed 8 July 2020). Accessed.
[34] A. Chiasera, O. Sayginer, E. Iacob, A. Szczurek, S. Varas, J. Krzak, O.S. Bursi, D. Zonta, A. Lukowiak, G.C. Righini, M. Ferrari, in: S. Taccheo, M. Ferrari, J. I. Mackenzie (Eds.), Fiber Lasers Glas. Photonics Mater. Through Appl. II, SPIE, 2020, p. 3.
[35] M. Bellingeri, A. Chiasera, I. Kriegel, F. Scotognella, Opt. Mater. 72 (2017) 403.
[36] F. Scotognella, A. Chiasera, L. Criante, E. Aluicio-Sarduy, S. Varas, S. Pelli, A. Łukowiak, G.C. Righini, R. Ramponi, M. Ferrari, Ceram. Int. 41 (2015) 8655.